MAGNETOHYDRODYNAMICS Vol. 39 (2003), No. 3, pp. 259–265

ON THE LOW-REYNOLDS-NUMBER MOTION OF A NON-CONDUCTING PARTICLE IN UNIFORM ELECTRIC AND MAGNETIC FIELDS

A. Sellier

LadHyX. Ecole polytechnique, 91128 Palaiseau Cedex, FRANCE

We present the formulation and the numerical implementation of a new boundary approach that permits us to compute the rigid-body motion of an arbitrarily-shaped, freely-suspended and non-conducting particle immersed in a liquid metal under the action of prescribed and uniform ambient electric and magnetic fields **E** and **B**. The paper describes the advocated numerical strategy and discusses preliminary benchmarks against the analytical solution obtained elsewhere for an ellipsoidal particle. The case of an insulating pear-shaped particle, which may experience both translation and rotation, is also briefly addressed.

Introduction. Under the application of uniform ambient electric and magnetic fields **E** and **B**, any solid and non-conducting particle freely suspended in a viscous liquid metal experiences a rigid-body motion [1]. Since this phenomenon may receive basic applications in impurities separation, it is of prime interest to determine the motion of a non-conducting, solid and arbitrarily-shaped particle, i.e., its angular velocity $\mathbf{\Omega}$ and translational velocity $\mathbf{U}$ (the velocity of one point, say O, attached to the particle). Within a relevant framework [2], it has been possible recently [3] to propose a suitable boundary formulationto to carry out this task. Contrary to [1, 4], which only deal with spheres (or cylinders), the advocated method holds for a particle of arbitrary geometry as soon as one succeeds in achieving a powerful numerical implementation. This paper both presents and tests such a suitable numerical strategy.

1. Governing system. This section briefly introduces our governing equations and for additional details the reader is directed to [3]. Henceforth, we adopt the Cartesian coordinates (O, x_1, x_2, x_3) and the usual tensor summation convention. For instance, $\mathbf{x} = x_i\mathbf{e}_i$, whereas $\mathbf{U} = U_j\mathbf{e}_j$ and $\mathbf{\Omega} = \Omega_j\mathbf{e}_j$. The particle $\mathcal{P}$ disturbs the applied field $\mathbf{E}$ so that the electric field in the fluid domain $\mathcal{D}$ becomes$\mathbf{E} - \nabla\phi$, where the perturbation potential ϕ obeys the well-posed exterior Neumann problem

$$\nabla^2\phi = 0 \text{ in } \mathcal{D}, \quad \nabla\phi \to \mathbf{0} \quad \text{as } \mathbf{x} \to \infty \text{ and} \quad \nabla\phi \cdot \mathbf{n} = \mathbf{E} \cdot \mathbf{n} \text{ on } S, \qquad (1)$$

with $\mathbf{n}$ being the unit outward normal on the insulating surface S of the particle. The liquid metal of constant viscosity μ, density ρ and electric conductivity σ experiences a quasi-steady Stokes flow $(\mathbf{u}, p)$ and the particle $\mathcal{P}$ has a volume $\mathcal{V}_\mathcal{P}$ and a small enough length scale a such that indeed $\mathrm{Re} = \rho V a/\mu \ll 1$, where V denotes the scale of $\mathbf{u}$. Let us introduce six steady Stokes flows $\mathbf{u}_T^{(i)}$ and $\mathbf{u}_R^{(i)}$, free from body forces and vanishing far from O, that are subjected to the following rigid-bodyboundary conditions

$$\mathbf{u}_T^{(i)} = \mathbf{e}_i, \quad \mathbf{u}_R^{(i)} = \mathbf{e}_i \wedge \mathbf{x} \quad \text{on } S. \qquad (2)$$

We further denote by $\mathbf{f}_T^{(i)}$ and $\mathbf{f}_R^{(i)}$ the surface stress arising on S in the above-mentioned flows $\mathbf{u}_T^{(i)}$ and $\mathbf{u}_R^{(i)}$. The knowledge of these forces provides the Cartesian components K_{ij}, W_{ij}, V_{ij} and D_{ij} of the so-called [5] translation, rotation and coupling second-rank tensors $\mathbf{K}, \mathbf{W}, \mathbf{V}$ and $\mathbf{D}$ so that

$$-\mu K_{ij} = \int_S \mathbf{e}_j \cdot \mathbf{f}_T^{(i)} \mathrm{d}S; \quad -\mu W_{ij} = \int_S [\mathbf{e}_j \wedge \mathbf{x}] \cdot \mathbf{f}_R^{(i)} \mathrm{d}S, \tag{3}$$

$$-\mu V_{ij} = \int_S [\mathbf{e}_j \wedge \mathbf{x}] \cdot \mathbf{f}_T^{(i)} \mathrm{d}S; \quad -\mu D_{ij} = \int_S \mathbf{e}_j \cdot \mathbf{f}_R^{(i)} \mathrm{d}S. \tag{4}$$

According to [3], the unknown velocity components U_j and Ω_j are then governed by the key linear 6-equation system

$$K_{ij}U_j + V_{ij}\Omega_j = \frac{1}{\mu}\Big\{ -\sigma \mathcal{V}_{\mathcal{P}} [\mathbf{E} \wedge \mathbf{B}] + \mathbf{F} \Big\} \cdot \mathbf{e}_i, \tag{5}$$

$$D_{ij}U_j + W_{ij}\Omega_j = \frac{1}{\mu}\Big\{ \sigma [\mathbf{E} \wedge \mathbf{B}] \wedge \Big[\int_{\mathcal{P}} \mathbf{x}\, \mathrm{d}v \Big] + \mathbf{G} \Big\} \cdot \mathbf{e}_i, \tag{6}$$

where $\mathcal{V}_{\mathcal{P}}$ designates the particle volume, and the vectors $\mathbf{F}$ and $\mathbf{G}$ are given by the relations

$$\mathbf{F} \cdot \mathbf{e}_i = \sigma \mathcal{L}[\mathbf{f}_T^{(i)}]/(8\pi\mu), \quad \mathbf{G} \cdot \mathbf{e}_i = \sigma \mathcal{L}[\mathbf{f}_R^{(i)}]/(8\pi\mu), \tag{7}$$

if the linear operator $\mathcal{L}$ is defined as:

$$\begin{aligned} \mathcal{L}[\mathbf{v}] = &- \int_S \int_S \mathbf{v}(P) \cdot [\nabla\phi(M) \wedge \mathbf{B}] \frac{\mathbf{PM} \cdot \mathbf{n}(M)}{PM} \mathrm{d}S_P \mathrm{d}S_M \\ &+ \int_S \int_S \Big[\mathbf{v}(P) \cdot \frac{\mathbf{PM}}{PM} \Big] \Big[\nabla\phi(M) \wedge \mathbf{B} \Big] \cdot \mathbf{n}(M)\, \mathrm{d}S_P\, \mathrm{d}S_M \\ &+ \int_S \int_S \epsilon_{kmn} PM [\mathbf{v} \cdot \mathbf{e}_k](P) [\mathbf{B} \cdot \mathbf{e}_n] [\phi_{,ml}(\mathbf{n} \cdot \mathbf{e}_l)](M)\, \mathrm{d}S_P\, \mathrm{d}S_M. \end{aligned} \tag{8}$$

In above equality (8), the symbol ϵ_{kmn} denotes the Cartesian component of the usual asymmetric permutation tensor and the notation $\phi_{,ml} = \partial^2\phi/\partial x_m \partial x_l$ is employed. Since its 6×6 square matrix is symmetric and positive-definite [6], governing system (5)–(6) admits a unique solution $(\mathbf{U}, \mathbf{\Omega})$. By virtue of relations (3)–(4), (7) and definition (8), the determination of $(\mathbf{U}, \mathbf{\Omega})$ solely requires to compute the previously mentioned surface forces $\mathbf{f}_T^{(i)}, \mathbf{f}_R^{(i)}$ and the first-order and second-order Cartesian derivatives of the perturbation potential ϕ on the insulating boundary S. In other words, the proposed formulation circumvents calculating the fluid flow $(\mathbf{u}, p)$ and the perturbation potential ϕ in the whole unbounded fluid domain $\mathcal{D}$; at least as soon as we are able to evaluate separately $\mathbf{f}_T^{(i)}, \mathbf{f}_R^{(i)}$ and the Cartesian derivatives $\phi_{,m}$ and $\phi_{,ml}$ on S.

2. Relevant boundary integral equations and numerical procedure. This key section presents three relevant boundary-integral equations on S that permits us to accurately compute the required quantities $\mathbf{f}_T^{(i)}, \mathbf{f}_R^{(i)}, \nabla\phi$ and $\phi_{,ml}$ on the particle surface. More precisely, we appeal to the following equations:

(1) One Fredholm boundary-integral equation of the first kind. As established in [7], for $L \in \{T, R\}$ the required surface forces on S obey the following integral equation

$$[\mathbf{u}_L^{(i)} \cdot \mathbf{e}_k](M) = -\int_S \Big\{ \frac{\delta_{jk}}{PM} + \frac{(\mathbf{PM} \cdot \mathbf{e}_j)(\mathbf{PM} \cdot \mathbf{e}_k)}{PM^3} \Big\} \Big[\frac{\mathbf{f}_L^i \cdot \mathbf{e}_j}{8\pi\mu} \Big](P) \mathrm{d}S_P, \quad k = 1, 2, 3 \tag{9}$$

where δ denotes a usual Kronecker Delta symbol. Actually, (9) not only holds on S but also within the whole fluid domain $\mathcal{D}$. Such simple single-layer representation of the velocity field $\mathbf{u}_L^{(i)}$ in $\mathcal{D}$ is due to a very specific nature (a rigid-body motion of S) of the prescribed boundary conditions (2).

(2) A widely-employed Fredholm boundary-integral equation of the first or second kind. If ψ is harmonic in $\mathcal{D}$ and vanishes far from O, the application of the Green's theorem yields the basic integral equation

$$A_M[\psi] = B_M[\nabla\psi \cdot \mathbf{n}] \quad \text{on} \quad S \tag{10}$$

with the following definitions:

$$A_M[\psi] = -4\pi\psi(M) + \int_S \Big[\psi(P) - \psi(M)\Big] \frac{\mathbf{PM} \cdot \mathbf{n}(P)}{PM^3} \, \mathrm{d}S, \tag{11}$$

$$B_M[\nabla\psi \cdot \mathbf{n}] = \int_S \frac{[\nabla\psi \cdot \mathbf{n}](P)}{PM} \, \mathrm{d}S. \tag{12}$$

Selecting $\psi = \phi$, the above integral-equation of the second kind (10) provides the numerical approximation of ϕ on the insulating surface S.

(3) A new Fredholm-boundary integral equation of the second kind. For ψ harmonic in $\mathcal{D}$, vanishing far from O, and of prescribed normal flux $\nabla\psi.\mathbf{n}$ on S, it has been possible to establish [8] in the following integral equation of the second kind

$$C_M^i[\nabla\psi] = D_M^i[\nabla\psi \cdot \mathbf{n}] \quad \text{on} \quad S \quad \text{for} \quad i \in \{1,2,3\} \tag{13}$$

where the operators C_M^i and D_M^i are defined as

$$D_M^i[\nabla\psi \cdot \mathbf{n}] = -I_i(M,S)(\nabla\psi \cdot \mathbf{n})(M) + \int_S \frac{\big[(\nabla\psi \cdot \mathbf{n})(P) - (\nabla\psi \cdot \mathbf{n})(M)\big]}{MP^3} (\mathbf{PM} \cdot \mathbf{e}_i) \, \mathrm{d}S, \tag{14}$$

$$I_i(M,S) = \int_S \left[\frac{\mathbf{MP} \cdot \mathbf{n}(P)}{MP^2} - \kappa(P)\right] \frac{\mathbf{n}(P) \cdot \mathbf{e}_i}{MP} dS, \quad \kappa(P) = \mathrm{div}_S\big[\mathbf{n}(P)\big], \tag{15}$$

$$C_M^i[\nabla\psi] = 2\pi\psi_{,i}(M) - \big[D_{ij}\psi\big](M) I_j(M,S) + \int_S \frac{\big[D_{ij}\psi(P) - D_{ij}\psi(M)\big]}{MP^3} (\mathbf{PM} \cdot \mathbf{e}_j) \, \mathrm{d}S, \tag{16}$$

with the tangential surface operators D_{ij}, so that

$$\big[D_{ij}\psi\big](M) = \big[\mathbf{n}(M) \cdot \mathbf{e}_i\big]\psi_{,j}(M) - \big[\mathbf{n}(M) \cdot \mathbf{e}_j\big]\psi_{,i}(M). \tag{17}$$

In view of the above results (10) and (13), we suggest to proceed as follows:

(i) We first compute $\nabla\phi$ on S by inverting (13) and taking into account boundary condition (1), i.e., the relation$\nabla\phi \cdot \mathbf{n} = \mathbf{E} \cdot \mathbf{n}$ on S.

(ii) Observing that $\phi_{,m}$ is harmonic in $\mathcal{D}$ and vanishes far from O, we then obtain the normal flux $\nabla[\phi_{,m}] \cdot \mathbf{n}$ on S from the previous knowledge of $\phi_{,m}$ by resorting again to (10). Selecting $\psi = \phi_{,m}$, we finally gain the required gradient $\nabla\phi_{,m}$ on S by inverting (13).

The advocated procedure, consisting of (i) and (ii), may appear cumbersome to the reader. For instance, one would perhaps think about first approximating

$\nabla\phi$ on S by tangential derivation of the computed value of ϕ and the knowledge of the normal derivative $\nabla\phi.\mathbf{n} = \mathbf{E}\cdot\mathbf{n}$ and further deduce, through an additional numerical differentiation, the derivatives $\phi_{,ml}$. Unfortunately, such a simple approach results in a poor accuracy, especially for the second-order derivatives $\phi_{,ml}$ that is dramatically damaging for the accurate estimation of the rigid-body motion $(\mathbf{U}, \mathbf{\Omega})$. The suggested method is free of this drawback: it yields accurate approximations of both $\phi_{,m}$ and $\phi_{,ml}$ on S.

Any encountered boundary-integral equation (9), (10) or (13) is discretized by using a N–node mesh of isoparametric, curvilinear and triangular 6-node boundary elements on the surface S. For details, regarding the implementation of such a widely-employed Boundary Element Method, the reader is directed to standard textbooks (see, for instance, [9]). Each discretized integral equation then becomes a linear matrix system $AX = Y$ of fully populated and asymmetric influence $N' \times N'$ square matrix A (with $N' = N$ for equation (10) and $N' = 3N$ for equations (9) and(13)). The solution is finally obtained by resorting to a Gaussian elimination.

3. Numerical comparisons for ellipsoidal particles. In order to ascertain both the validity and the accuracy of the advocated numerical strategy, it is essential to compare, whenever possible, the computed velocity components U_j and Ω_j with theoretical predictions. Fortunately, the solution has been recently derived in the closed form [3] for any insulating ellipsoidal particle, and such simple geometry, therefore, appears as a natural candidate for numerical benchmarks. Since it is orthotropic, i.e., it admits three orthogonal planes of symmetry through its centre of volume, the ellipsoid does not rotate [2]. If the particle $\mathcal{P}$ admits the equation

$$\frac{x_1^2}{a_1^2} + \frac{x_2^2}{a_2^2} + \frac{x_3^2}{a_3^2} \leq 1, \tag{18}$$

its translational velocity $\mathbf{U}$ is found to be [3]

$$\mathbf{U} = \frac{\sigma}{\mu}\frac{\epsilon_{ijk}}{12}\left\{\frac{\alpha_j(2a_j^2 + \alpha_i a_i^2)}{[\alpha_j - 2]} - \alpha_i a_i^2\right\}[\mathbf{E}\cdot\mathbf{e}_j][\mathbf{B}\cdot\mathbf{e}_k]\mathbf{e}_i \tag{19}$$

with the following definitions

$$\alpha_i = a_1 a_2 a_3 \int_0^\infty \frac{(a_i^2 + t)^{-1} dt}{\{(a_1^2+t)(a_2^2+t)(a_3^2+t)\}^{1/2}}, \quad \Delta(t) = \sqrt{\Xi(t)}. \tag{20}$$

For a spheroid with $a_1 = a_2 = a$ and $a_3 = \lambda a$, it is possible by elementary algebra to express the above coefficients α_i in the closed form. Under such circumstances, one indeed easily arrives at [3]

$$\alpha_1 = \alpha_2 = \frac{\lambda^2}{\lambda^2 - 1}\left[1 - \frac{\chi'}{2\lambda^2}\right], \quad \alpha_3 = \frac{1}{\lambda^2 - 1}\left[\chi' - 2\right], \tag{21}$$

$$\chi'(\lambda) = \frac{\lambda}{\sqrt{\lambda^2 - 1}} \log\left[2\lambda^2 + 2\lambda\sqrt{\lambda^2 - 1} - 1\right] \text{ if } \lambda > 1, \tag{22}$$

$$\chi'(\lambda) = \frac{2\lambda}{\sqrt{1-\lambda^2}} \arctan\frac{\sqrt{1-\lambda^2}}{\lambda} \quad \text{if} \quad \lambda < 1. \tag{23}$$

For a sphere of radius a one immmediately recovers the well-known and simple result [1]

$$\mathbf{U} = -\frac{\sigma a^2}{6\mu}[\mathbf{E} \wedge \mathbf{B}]. \tag{24}$$

Table 1. Effect of mesh refinement for a sphere of radius a if $\mathbf{E} = E\mathbf{e}_2$ and $\mathbf{B} = B\mathbf{e}_1$.

N	74	242	530	1058
$\mu U_3/[\sigma a^2 EB]$	0.17486	0.16765	0.16709	0.16675
$\mu U_3^{\text{th}}/[\sigma a^2 EB]$	0.16667	0.16667	0.16667	0.16667

For example, if $\mathbf{E} = E\mathbf{e}_2$ and $\mathbf{B} = B\mathbf{e}_1$ with $EB \neq 0$, the theoretical velocity reads $\mathbf{U} = U_3^{\text{th}}\mathbf{e}_3$ with $\mu U_3^{\text{th}}/[\sigma a^2 EB] = 0.16667$.

Our computed and normalized velocity components $\mu\Omega_j/[\sigma a\, EB]$, $\mu U_1/[\sigma a^2 EB]$ and $\mu U_2/[\sigma a^2 EB]$ are weaker than 10^{-4}, whereas, as reported in Table 1, the non-zero computed component U_3 is found to exhibit a nice convergence towards its theoretical value U_3^{th}, as the number N of collocation points increases. The choice of 1058 collocation points yields a 4-digit accuracy for spheres.

For oblate ($\lambda < 1$) or prolate ($\lambda > 1$) spheroidal particles, equation (19) shows that $\mathbf{U}$ is unnecessarily parallel to $\mathbf{E} \wedge \mathbf{B}$ and strongly depends upon the particle orientation relative to $\mathbf{E}$ and $\mathbf{B}$.

The non-zero normalized velocity components $\mu U_k/[\sigma a^2 EB]$ are computed for different settings $\mathbf{E} = E\delta_{im}\mathbf{e}_m$ and $\mathbf{B} = B\delta_{jm}\mathbf{e}_m$ using the refined 1058–node and compared to the theoretical values given by (19) and (21)–(23) both for oblate ($\lambda < 1$) and prolate ($\lambda > 1$) spheroids. Again, a 4-digit accuracy is observed and clearly the spheroid translation is very sensitive to the ambient electric and magnetic fields. In summary, the use of about one thousand collocation points on the surface of moderately prolate or oblate spheroids makes it possible to obtain very accurate estimates of the rigid-body motion. As the spheroid collapses to a thin disk or becomes slender and needle-shaped, it is of course necessary to resort to more and more refined meshes on the surface of the particle but the present method permits us to deal at a reasonable cpu cost with a wide class of ellipsoidal particles (not too thin or too slender ones).

4. Case of an insulating and pear-shaped particle. As established in [2], non-orthotropic and axisymmetric particles may experience both translation and rotation. As a simple example of such bodies, we consider a pear-shaped particle, which has $(O, \mathbf{e}_3)$ as the axis of symmetry. More precisely, the selected surface S admits the equation $\sqrt{x_1^2 + x_2^2} = ah(x_3/a)$, where the positive function h obeys

Table 2. Comparison for a refined 1058–node mesh between the computed and the theoretical normalized velocity components $\mu U_k/[\sigma a^2 EB]$ for either oblate ($\lambda < 1$) or prolate ($\lambda > 1$) spheroids and different settings $(\mathbf{E}, \mathbf{B}) = (E\mathbf{e}_i, B\mathbf{e}_j)$ with $EB \neq 0$.

λ	(i,j)	k	$\mu U_k/[\sigma a^2 EB]$	$\mu U_k^{\text{th}}/[\sigma a^2 EB]$
1/2	(2,1)	3	0.08046	0.08036
1/2	(2,3)	1	−0.10329	−0.10320
1/2	(3,2)	1	0.13018	0.12979
$\sqrt{2}$	(2,1)	3	0.23269	0.23257
$\sqrt{2}$	(2,3)	1	−0.20164	−0.20152
$\sqrt{2}$	(3,2)	1	0.19236	0.19235

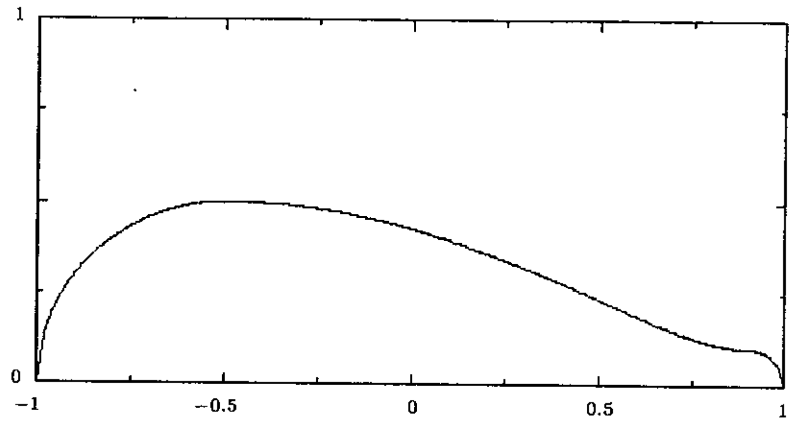

Fig. 1. Selected profile function h for a pear-shaped particle.

$$h^2(u)=u(1-u) \text{ if } -1 \le u < -0.5,\ h^2(u)=1.8u-u^2-0.8 \text{ if } 0.9 < u \le 1, \quad (25)$$

$$h^2(u) = 0.01 + 0.12\left\{1 - \sin\left[\frac{\pi}{1.4}(u-0.2)\right]\right\} \quad \text{if } -0.5 \le u \le 0.9. \quad (26)$$

The above function h is plotted in Fig. 1 versus the normalized coordinate $u = x_3/a$ and our insulating particle is clearly far from being orthotropic. As shown in Table 3, this pear-shaped particle both translates and rotates for $\mathbf{E} = E\mathbf{e}_2$ and $\mathbf{B} = B\mathbf{e}_3$ (with $EB \neq 0$). In addition, it has been found that for $\mathbf{E} = E\mathbf{e}_2$ and $\mathbf{B} = B\mathbf{e}_1$ $\mathbf{U}$ and $\boldsymbol{\Omega}$ are parallel to $\mathbf{e}_3$ and $\mathbf{e}_2$, respectively. Accordingly, for the setting $(\mathbf{E}, \mathbf{B}) = (E\mathbf{e}_2, B\mathbf{e}_3)$ the pear-shaped particle translates normal to $\mathbf{e}_2$ and rotates about the $\mathbf{e}_2$ direction ($\boldsymbol{\Omega}$ is aligned with $\mathbf{e}_2$). The orientation of the particle, therefore, changes with time and its rigid-body motion thus becomes time-dependent.

Concluding remarks. As evidenced by the discussed benchmarks against the available analytical solution for the insulating ellipsoid, the proposed procedure makes it possible to accurately compute the required rigid-body motion of a non-conducting particle at a reasonable cost (one only needs to discretize the insulating surface of the particle). Like any other orthotropic particle [2], ellipsoidal particles, however, only translate. By contrast, a non-conducting and pear-shaped particle has been found to experience a rotation, which is dramatically sensitive to the orientation of the ambient electric and magnetic fields $\mathbf{E}$ and $\mathbf{B}$.

Table 3. Effect of mesh refinement on the non-zero normalized Cartesian velocity components for a pear-shaped particle if $\mathbf{E} = E\mathbf{e}_2$ and $\mathbf{B} = B\mathbf{e}_3$.

N	170	458	1874
$\mu U_1/[\sigma a^2 EB]$	−0.0487	−0.0492	−0.0478
$\mu \Omega_2/[\sigma a EB]$	0.0118	0.0115	0.0107

Finally, one should point out that in practice solid impurities may be conducting. It would be nice in the future to extend the present work to the case of an arbitrarily-shaped and conducting solid particle. Such a challenging issue is under current investigation.

REFERENCES

1. D. Leenov and A. Kolin. Theory of electromagnetophoresis. I. Magnetohydrodynamic forces experienced by spherical and symmetrically oriented cylindrical particles. *J. Chem. Phys*, vol. 22 (1954), pp. 683–688.
2. H. K. Moffatt and A. Sellier. Migration of an insulating particle under the action of uniform ambient electric and magnetic fields. Part 1. General theory. *J. Fluid Mech.*, vol. 464 (2002), pp. 279–286.
3. A. Sellier. Migration of an insulating particle under the action of uniform ambient electric and magnetic fields. Part 2. Boundary formulation and ellipsoidal particles. *Accepted at J. Fluid Mech.*
4. P. Marty and A. Alemany. Theoretical and experimental aspects of electromagnetic separation. In: *Metallurgical Applications of Magnetohydrodynamics* (ed. H. K. Moffatt & M. R. E. Proctor). Metals Society. (1984), pp. 245–259.
5. S. Kim and S. J. Karrila. Microhydrodynamics: principles and selected applications. 1991, Butterworth.
6. J. Happel and H. Brenner. Low Reynolds number hydrodynamics. 1973, Martinus Nijhoff.
7. C. Pozrikidis. Boundary integral and singularity methods for a linearized viscous flow. 1992, Cambridge University Press.
8. A. Sellier. On the numerical approximation of the derivatives of potentials on the smooth and simply or multiply connected boundary by using boundary-integral equations. *Submitted to Proc. R. Soc. Lond. A.*
9. M. Bonnet. Boundary integral equations methods for solids and fluids. 1999, John Wiley & Sons Ltd.

Received 03.04.03